Highly Conductive Vertically Aligned Carbon Nanotubes Grown on $Mg_{0.3}Zn_{0.7}O$ Thin Film Template Using Thermal Chemical Vapour Deposition Method

Muhamad Salina[*], Mohamad Hafiz Mamat, Suriani Abu Bakar[1], Rafidah Ahmad, Yosri Mohd Siran[2],
Syahril Anuar M. Rejab[2], Ahmad Jais Asis[2], Shaharudin Tahiruddin[2], and Mohamad Rusop

NANO ElecTronic Centre, Faculty of Electrical Engineering, Universiti Teknologi MARA, 40450 Shah Alam, Selangor, Malaysia
[1]*NANO SciTech Centre, Faculty of Science, Universiti Teknologi MARA, 40450 Shah Alam, Selangor, Malaysia*
[2]*Sime Darby Research Sdn. Bhd., Pulau Carey, Klang 41400, Selangor, Malaysia*

Novel vertically aligned carbon nanotubes (VACNTs) were successfully grown on $Mg_{0.3}Zn_{0.7}O$ thin film template. Current–voltage (I–V) characteristics of both VACNTs and VACNTs/$Mg_{0.3}Zn_{0.7}O$ were measured where it first demonstrates that highly conductive VACNTs with more than $1 \times 10^5\,S\,cm^{-1}$ were achieved using $Mg_{0.3}Zn_{0.7}O$ thin film template, though both samples showing only a small difference in the micro-Raman spectroscopy. This suggested that the used of $Mg_{0.3}Zn_{0.7}O$ thin film template is capable of promoting the growth of VACNTs to have a smaller diameter and blocked the electrons' penetration into silicon that leads to highly conductive sample.

© 2011 The Japan Society of Applied Physics

1. Introduction

A carbon nanotubes (CNTs) is one of the well known conductive material. It has been used and being optimized as a filler to improve the conductivity of other materials especially in polymer.[1–3] Furthermore, the outstanding characteristics of CNTs itself make it possible to be used in a broad range of applications especially in electronics devices such as field effect transistor (FET),[4] field emission display (FED),[5] sensors,[6] diodes,[7] etc.

The growth of CNTs on silicon substrate mostly was assisted by many types of catalysts such as ferrocene,[8] cobalt,[9] nickel,[10] etc.; whether as seeded or as floating catalyst. As the corollary, the resultant grown CNTs will be widely differ in their length, as well as the tube diameter, that will give totally different characteristics especially to the physical and electrical properties. A thorough study and investigation should be handled to understand the characteristics of resultant CNTs.

Since a lot of papers has been reported about the use of CNTs as a filler, highlighting the successfulness in increasing the conductivity of other materials, we, in the other way attempt to increase the conductivity of the CNTs itself that might be useful for broader applications, mainly in FET, where a highly conductive material is needed to act as a channel that can permit electrons to flow from source to drain. At present, there is less report regarding to this matter that motivates us to pursue on this study in further depth. Therefore, in this paper, we report the growth of vertically aligned CNTs (VACNTs) that exhibits high conductivity, which was firstly achieved using $Mg_{0.3}Zn_{0.7}O$ thin film template. The mentioned template is needed in FET structure in order to have a semi-insulating material with resistivity of more than $10^6\,\Omega\,cm$ that can act as a buffer layer, without changing the hexagonal structure of the thin film.[11] Moreover, the used of MgO and ZnO has been reported earlier as a catalyst[12–17] on the growth of CNTs. By using $Mg_{0.3}Zn_{0.7}O$ thin film as a template, with the advantage of containing both MgO and ZnO in one thin film, it indirectly act as a co-catalyst, where we addressed VACNTs forest with lesser diameter was achieved when we compared the resultant VACNTs with the bare VACNTs, the one without any template used. The synthesis process was done to analyze both samples.

2. Experimental Procedure

2.1 $Mg_{0.3}Zn_{0.7}O$ thin film preparation

Sol–gel method and spin coating technique was employed to deposit $Mg_{0.3}Zn_{0.7}O$ thin film on silicon with orientation of [100]. Silicon with the dimension of $2\,cm^2$ was cleaned with hydrofluoric acid and de-ionized water with the ratio of $1:10$ in an ultrasonic bath for 10 min. Then, the silicon was gently washed and rinsed with deionized water. This is to make sure that no unwanted particles on the silicon surface presence and will indirectly contaminate the samples, as any contamination will degrade the performance and influenced the growth of $Mg_{0.3}Zn_{0.7}O$ thin film.

The starting material used was zinc acetate dihydrate $[Zn(CH_3COO)_2 \cdot 2H_2O$; Riedel-de Haen], together with solvent, 2-methoxyethanol $[C_3H_8O_2$; Sigma-Aldrich], mono-ethanolamine $[C_2H_7NO$; Merck] as a stabilizer and magnesium nitrate hexahydrate $[Mg(NO_3)_2 \cdot 6H_2O$; Systerm] as a dopant. The solution of 0.4 M was stirred and heated at $60\,°C$ for 2 h. This process was continued for aging purpose, which took part for 24 h at room temperature.

The deposition of the thin film was done using a spin coater in Ar gas ambient (4 mbar, 0.5 l/min). In order to get a thin film with appropriate thickness, five layers were coated with spinning speed of 3000 rpm for 60 s. Each layer of 10 drops sol was pre-heated at $150\,°C$ for 10 min. The thin film was annealed at $550\,°C$ before being used as a template to grow VACNTs.

2.2 Synthesis of CNTs

CNTs were synthesized using thermal chemical vapour deposition (TCVD) method. Using palm oil mixed ferrocene as a precursor for CNTs,[18] it was placed in an alumina boat and transferred into a horizontal quartz tube in the first column of a double furnace heater. The target, $Mg_{0.3}Zn_{0.7}O$ thin film template was placed in the same quartz tube, at the second reactor, with heating temperature of $800\,°C$. The deposition process was done in the duration of 30 min with Ar as a carrier gas. The same procedure was employed to deposit CNTs on bare silicon substrate without any template used.

*E-mail address: ina1320@yahoo.com
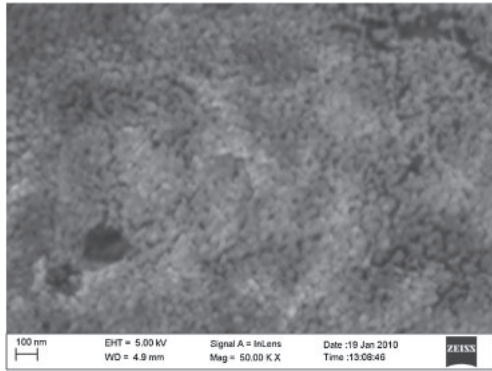
Fig. 1. FESEM images of $Mg_{0.3}Zn_{0.7}O$ thin film template.

Fig. 2. XRD spectra of $Mg_{0.3}Zn_{0.7}O$ thin film template.

Fig. 3. Linear plot of resistivity versus Mg contents.

2.3 Characterization of the template and CNTs

The template was characterized by field emission scanning electron microscope (FESEM; ZEISS Supra 40VP) and X-ray diffraction (XRD; Rigaku Ultima IV) to inspect the surface morphology and the crystallinity, respectively. On the other hand, the product, VACNTs were then characterized by scanning electron microscope (SEM; JEOL JSM-360L) and FESEM to investigate the surface morphology, while micro-Raman spectroscopy (Horiba Jobin Yvon DU420A-OE-325) was used to inspect the crystal orientation. The material composition of the sample has been verified using an energy dispersive X-ray spectrometer (EDS) that was attached to a Zeiss Supra 40 VP FESEM. In order to examine the electrical properties, Keithley 2400 current–voltage (*I–V*) measurement system was adopted where gold was sputtered on top of the sample to perform as an electrode. Two probes system being used to measure the electrons movement from two electrodes of $1\,mm^2$ each. The gap between electrodes is 1 mm while the thickness of electrodes is 60 nm. With the support of $Mg_{0.3}Zn_{0.7}O$ thin film template as a buffer layer, it is expected that less electrons will be penetrated into silicon, resulting in less resistance path.

3. Results and Discussion

Surface morphology of $Mg_{0.3}Zn_{0.7}O$ thin film template is shown in Fig. 1, revealing the nanoparticles formed with the average diameter of 55 nm, while Fig. 2 shows the XRD analysis of the thin film. Because of the ionic radius of Mg^{2+} (0.78 Å) is comparable to that of Zn^{2+} (0.83 Å), so that the dimension of their crystal cells is very close to each other.[11] This can be seen in the XRD pattern where the peak is closed to ZnO peak, showing that it retains the hexagonal wurtzite structure of ZnO, parallel with the result found by Meher *et al.* in their study.[19] Three peaks were observed at the position of (100), (002), and (101), where the most intense peak was at (101). They also emphasized that the surface becomes rougher with the progress of Mg substitution in the thin film, which suitable to be used as a catalyst, which also true with our findings. The graph plot in Fig. 3 shows the rising in resistivity with the progress of Mg substitution in $Mg_xZn_{1-x}O$ thin film, where we had found out that with $x = 0.3$, the resistivity needed in FET applications was achieved without changing the phase of the thin film.
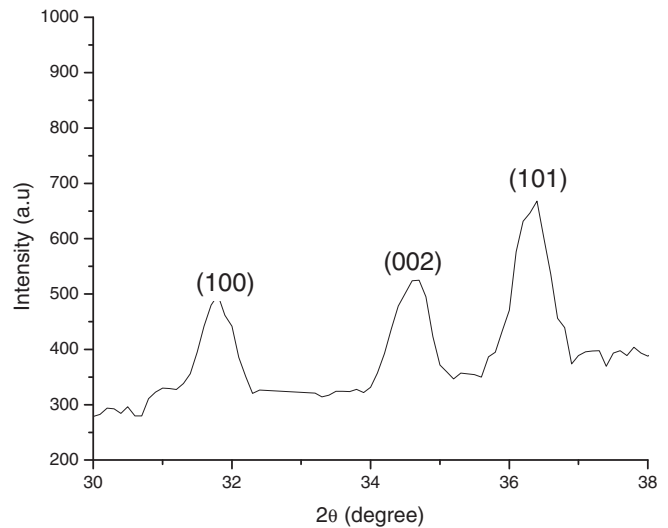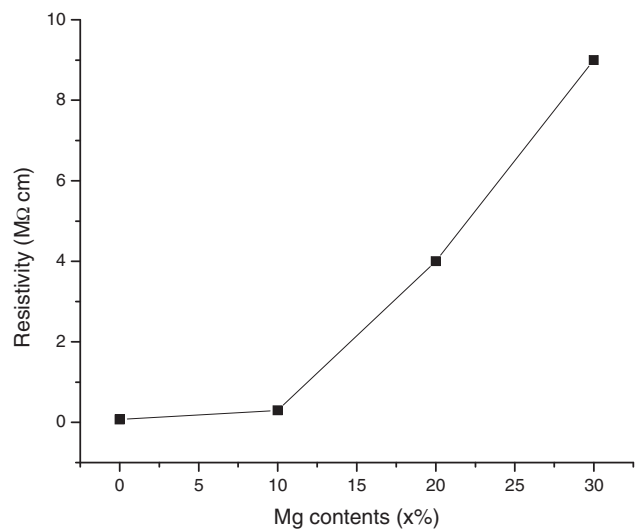
CNTs are produced from thermal decomposition of carbon from palm oil mixed ferrocene used over the surface of target, containing template or without template. Ferrocene molecules will decompose into nanosized Fe particles, whilst the palm oil molecules will decompose into a rich potion of hydrocarbons when being heated at 450 °C. Then, both hydrocarbon and nanosized Fe particles will mix and settled on the target. Minute temperature fluctuations due to Ar gas flow in the deposition tube resulted in the condensation of the dissolved carbon to nanotubes at the nanosized Fe particles.[18] This can be seen in SEM images where it shows that aligned CNTs in vertical direction were formed on both bare silicon (sample A) and on $Mg_{0.3}Zn_{0.7}O$ thin film template (sample B). Figures 4(a) and 4(b) show the VACNTs grown on bare silicon (being peeled off) where the length of the VACNTs was found to be in the average of $100\,\mu m$, while the diameter was in the average of 34 nm. The VACNTs' height is quite similar to the VACNTs grown on $Mg_{0.3}Zn_{0.7}O$ thin film template as shown in Fig. 4(c), showing that the decomposition of carbon was at the same rate for both samples.
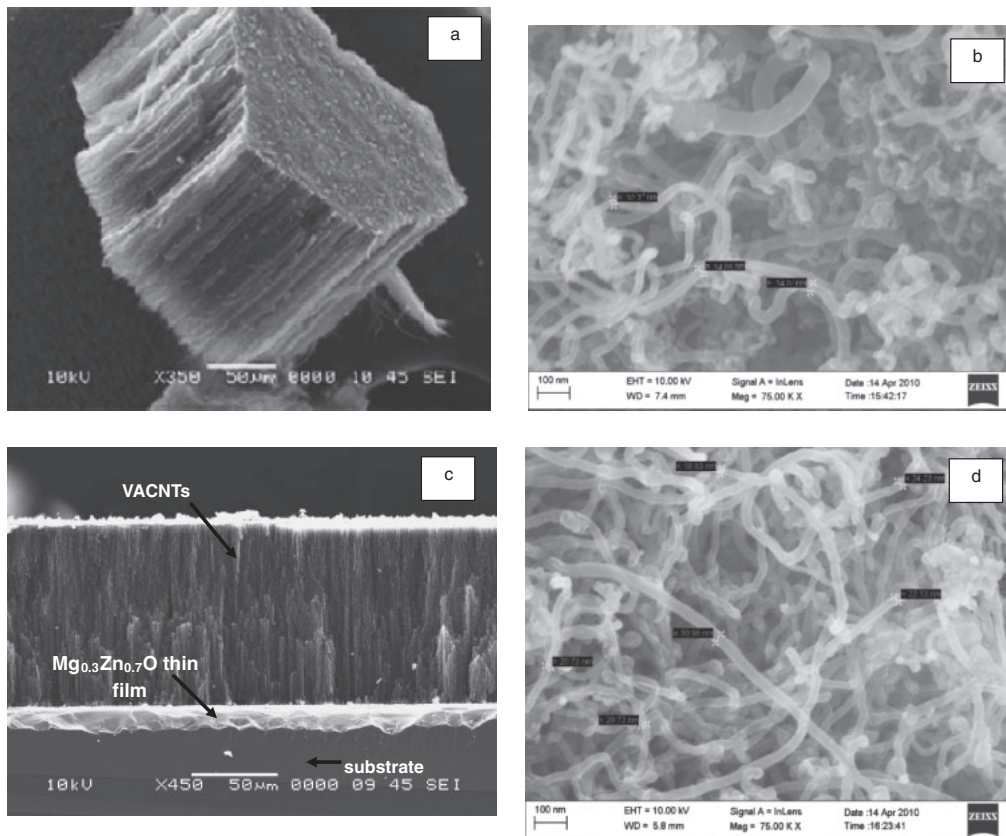
Fig. 4. SEM and FESEM images of VACNTs grown on bare silicon (a, b) and on $Mg_{0.3}Zn_{0.7}O$ thin film template (c, d).
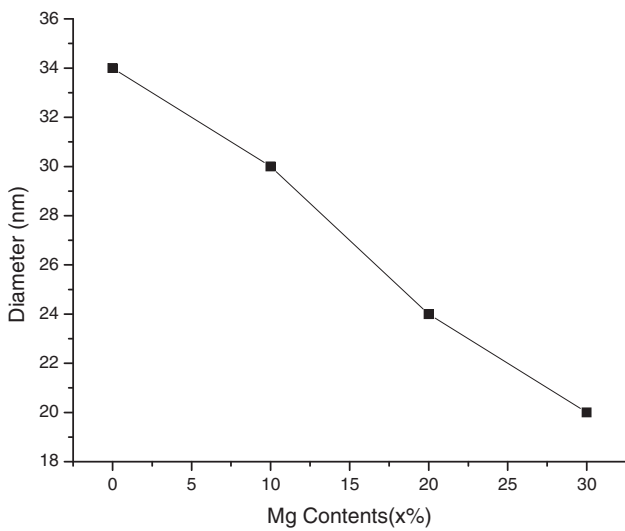
Fig. 5. Linear plot of CNTs' diameter versus Mg contents.

The effect of the template used can clearly be seen on the surface morphology of both samples, where the decreasing in a diameter size of CNTs was observed in Fig. 4(d). The decreasing of CNTs' diameter is proportional to the Mg contents in the thin film template where at least, the significance difference of 14 nm can be observed from the graph plot in Fig. 5 when both samples are being compared. Further inspection shows that the diameter of CNTs is gradually decreasing with the progress of Mg substitution in

$Mg_xZn_{1-x}O$ thin film where at $x = 0.1$, the average diameter of CNTs is 30 nm, compared to when $x = 0.0$, the average diameter is 4 nm larger. Further substitution of Mg resulted in lesser diameters where the average diameter is 24 and 20 nm at $x = 0.2$ and 0.3, respectively. It has been proven and well known that the diameter of the nanotubes is closely related to the size of the metal nano-particles present on the catalyst support i.e., template used.[20] Speculating this mechanism process, by heating the template at high degree of 750 °C, Zn and Mg at the surface of $Mg_{0.3}Zn_{0.7}O$ thin film template vapor due to its low melting point, where it has facilitated ferrocene to reduce the diameter of the particles formed, so that they can easily dissolve the carbon and also diffuse into the nanotube.[21] We also speculated that the migration rate of Fe, Zn and Mg nanoparticles on the template surface resulting in significant agglomeration of those particles, where in a special way has enhanced the catalytic activity across the template surface to become more stable and uniform, contributed to smaller diameter of CNTs produced. These findings are close agreement with some authors where they in their report had highlighted the used of MgO and ZnO as a catalyst for CNTs' growth.[12–17] Figure 6 shows the EDS spectrum revealing the composition of sample B, where the peak of carbon was found with atomic percent of 96.85 as compared to other material composition, indicating a high purity nanotubes has been produced. It also reveals the existence of catalysts used in the sample, which were Fe, Mg, and Zn, confirming the contribution of those catalysts to the growth of VACNTs.
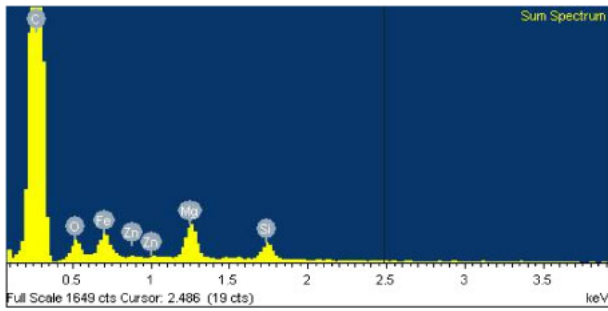
Fig. 6. (Color online) EDS spectrum of sample B.
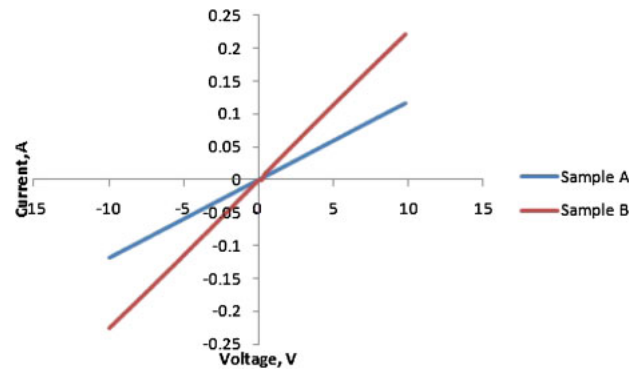
Fig. 8. (Color online) *I–V* response of VACNTs.

Table I. Average conductivity and resistivity.

Sample	Conductivity $(kS\,cm^{-1})$	Resistivity $(\mu\Omega\,cm)$
A	42.37	23.6
B	106.84	9.36
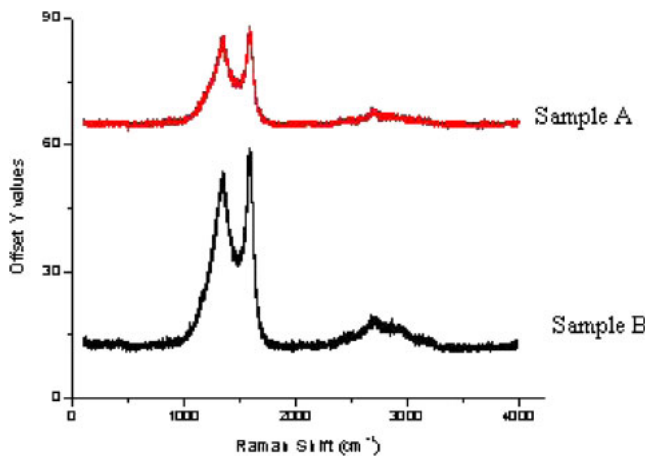
Fig. 7. (Color online) Raman spectroscopy showing D and G line for MWCNTs.

The crytallinity of the grown VACNTs was evaluated by micro-Raman spectroscopy. Figure 7 shows the Raman shift for both sample A and sample B. Both spectra show two broad bands at $1589\,cm^{-1}$ (G-band) and $1350\,cm^{-1}$ (D-band), where it substantiate that the grown VACNTs are multi-walled type as being reported elsewhere.[18] In general, the intensity of the D-band indicates the defect, impurities or lattice distortion in CNTs, while the G-band represent the degree of crystallinity in the graphite structure. The ratio of the intensities of these peaks, I_D/I_G for sample A was 0.9 while for sample B, it was found to be at 0.86, showing a slightly lower defect with the used of $Mg_{0.3}Zn_{0.7}O$ thin film template. Meanwhile, the G′ peak was found to be broad since the produced CNTs was mainly multi-walled CNTs. At sample B, highest intensity of G′ peak with lowest full width at half maximum (FWHM) were seen, where it perfectly matched with smaller diameter of the tube produced. The analysis from FESEM and micro-Raman spectroscopy was consistent where higher yield and good quality CNTs is at sample B.

The electrical properties were measured using Keithley 2400, which indicates that the conductivity of the VACNTs is directly proportional to the voltage applied. Because of the diameter reduction in the grown VACNTs on $Mg_{0.3}Zn_{0.7}O$ thin film template, the transfer of electrons between the carbon nanotubes becomes more efficient. This will resulted in more conductive sample as observed in the *I–V* response as shown in Fig. 8. At 10 V, a drastic increment of currents

was observed from 0.08 to 0.22 A. With this, we speculate that since the diameter of CNTs is quite large in sample A, a particle behave as if it were free when the confining dimension is large. However, as the diameter become smaller as in sample B, the confining dimension decreases, where the free carriers are being squeezed into a dimension that approaches a critical quantum measurement.[22] Hence, the smaller diameter CNTs exhibits quantum confinement effect characteristics in one-dimensional (1D) structure. Quantum confinement effect in 1D structure would improve a carrier transport or mobility.[22] This condition will lead to less leakage current in a tube during electrons' transportation. Furthermore, the use of $Mg_{0.3}Zn_{0.7}O$ thin film template as a buffer layer has blocked the electrons' penetration into silicon. This phenomenon will resulted in more efficient electrons movement with less resistance where electrons will jump to the next tube at the root in order to complete the path cycle. The current flow will be affected if the electrons are able to penetrate into the silicon during the cycle because of the path will be having a quite high resistance due to the silicon's properties. This is true with the Ohm's Law, where a high resistance in a path cycle will result in a low current flow as being observed in sample A. Moreover, as been discussed earlier, sample B has shown slightly less defect, more crystalline compared to sample A, consequently the movement of electrons will not be disturbed by amorphous carbon that indirectly will reduced the conductivity of the sample as the amorphous carbon is in the group of diamond, exhibit low conductivity property.[23]

With the average thickness of $100\,\mu m$, the conductivity and the resistivity of the sample can be calculated. Observing the data from Table I, the most conductive sample is sample B, which gives the conductivity of $106.84\,kS\,cm^{-1}$ and the resistivity of $9.36\,\mu\Omega\,cm$. The resulted conductivity is 10 times greater than reported by Kenneth *et al.*[24] which was $10\,kS\,cm^{-1}$.

4. Conclusions

Highly conductive VACNTs grown on $Mg_{0.3}Zn_{0.7}O$ thin film template have been successfully synthesized. The electrical properties showed that the sample become more conductive when the CNTs' diameter become smaller, due to the quantum confinement effect that leads to better electron transportation. The $Mg_{0.3}Zn_{0.7}O$ thin film template had supported the growth of the VACNTs, which caused the reduction in CNTs diameter by facilitated ferrocene to reduce the diameter of particles' formed and enhanced the catalytic activity. It can be concluded that sample B is highly conductive as compared to sample A, which can be employed to many electronics devices especially in FET applications. The simplicity in the sample preparation makes this as a significant potential to be applied in many electronics devices fabrication.

1) H. Koerner, W. Liu, M. Alexander, P. Mirau, H. Dowty, and R. A. Vaia: Polymer **46** (2005) 4405.
2) D. Zhang, K. Ryu, X. Liu, E. Polikarpov, J. Ly, M. E. Thompson, and C. W. Zhou: Nano Lett. **6** (2006) 1880.
3) I. D. Rosca and S. V. Hoa: Carbon **47** (2009) 1958.
4) L. Marty, V. Bouchiat, C. Naud, M. Chaumont, T. Fournier, and A. M. Bonnot: Nano Lett. **3** (2003) 1115.
5) N. S. Lee, D. S. Chung, I. T. Han, J. H. Kang, Y. S. Choi, H. Y. Kim, S. H. Park, Y. W. Jin, W. K. Yi, M. J. Yun, J. E. Jung, C. J. Lee, J. H. You, S. H. Jo, C. G. Lee, and J. M. Kim: Diamond Relat. Mater. **10** (2001) 265.
6) Y. Lu, C. Partridge, M. Meyyappan, and J. Li: J. Electroanal. Chem. **593** (2006) 105.
7) H. M. Manohara, E. W. Wong, E. Schlecht, B. D. Hunt, and P. H. Siegel: Nano Lett. **5** (2005) 1469.
8) M. S. Mohlala, X. Y. Liu, M. J. Witcomb, and N. J. Coville: Appl. Organomet. Chem. **21** (2007) 275.
9) J. Li, C. Papadopoulos, J. M. Xu, and M. Moskovits: Appl. Phys. Lett. **75** (1999) 367.
10) T. D. Makris, L. Giorgi, R. Giorgi, N. Lisi, and E. Salernitano: Diamond Relat. Mater. **14** (2005) 815.
11) A. Ohtomo, M. Kawasaki, T. Koida, K. Masabuchi, H. Koinuma, Y. Sakurai, Y. Yoshida, T. Yasuda, and Y. Segawa: Appl. Phys. Lett. **72** (1998) 2466.
12) G. Y. Xiong, D. Z. Wang, and Z. F. Ren: Carbon **44** (2006) 969.
13) R. Bonadiman, M. D. Lima, M. J. de Andrade, and C. P. Bergmann: J. Mater. Sci. **41** (2006) 7288.
14) S. C. Lyu, B. C. Liu, S. H. Lee, C. Y. Park, H. K. Kang, C. W. Yang, and C. J. Lee: J. Phys. Chem. B **108** (2004) 1613.
15) J. F. Colomer, C. Stephen, S. Lefrant, G. V. Tendeloo, I. Willems, Z. Konya, A. Fonseca, C. Lauren, and J. B. Nagy: Chem. Phys. Lett. **317** (2000) 83.
16) S. F. Lee, Y. P. Chang, and L. Y. Lee: J. Vac. Sci. Technol. B **26** (2008) 1765.
17) D. Xin, H. B. Zhang, G. D. Lin, Y. Z. Yuan, and K. R. Tsai: Catal. Lett. **85** (2003) 237.
18) A. B. Suriani, A. A. Azira, S. F. Nik, R. M. Nor, and M. Rusop: Mater. Lett. **63** (2009) 2704.
19) S. R. Meher, K. P. Biju, and M. K. Jain: J. Sol–Gel Sci. Technol. **52** (2009) 228.
20) D. Lupu, A. R. Biris, F. Watanabe, Z. R. Li, E. Dervishi, V. Saini, Y. Xu, A. S. Biris, M. Baibarac, and I. Baltog: Chem. Phys. Lett. **473** (2009) 299.
21) J. Sengupta and C. Jacob: J. Cryst. Growth **311** (2009) 4692.
22) S. Ilani and P. L. McEuen: Annu. Rev. Condens. Matter Phys. **1** (2010) 1.
23) Y. V. Preskov, Y. E. Evstefeeva, M. D. Krotova, V. V. Elkin, A. M. Baranov, and A. P. Dement'ev: Diamond Relat. Mater. **8** (1999) 64.
24) B. K. Kenneth, S. Charenjeet, M. Chhowalla, and W. I. Milne: Encycl. Nanosci. Nanotechnol. **1** (2004) 665.